ingegneria sismica
International Journal of Earthquake Engineering
Anno XLIII - Num. 2 - 2026

Fault detection and characterization of generator excitation system based on improved deep belief network

Zhebo Zhang[1,2], *Yanxiang Chen*[3], *Lihang Zhao*[1,2], *Qingfeng Cai*[4], *Mengfei Xiu*[1,2], *Pengyu Wang*[1,2,*] *and Hao Qin*[5]

[1] Zhejiang Energy R & D Institute Co. Ltd, Hangzhou, Zhejiang, 311121, China
[2] Key Laboratory of Energy Conservation & Pollutant Control Technology for Thermal Power of Zhejiang Province, Hangzhou, Zhejiang, 311121, China
[3] China Energy Engineering Group Zhejiang Electric Power Design Institute Co., Ltd, Hangzhou, Zhejiang, 310012, China
[4] Zhejiang Energy Jiahua Electric Power Generation Co., Ltd, Jiaxing, Zhejiang, 314201, China
[5] NR Electric Co., Ltd, Nanjing, Jiangsu, 211102, China

SUMMARY: *The excitation system is an important control equipment of synchronous generator, which plays an important role in the stable operation of synchronous generator and the whole power system. For this target, the article at first gives out the structure and working principle of the excitation system. After that, a classification method of faults which is established on wavelet packet decomposition is being studied. Furthermore, many signal handling methods are utilized by people to obtain the feature properties of malfunction signals that are connected with generator excitation system wrong operations. Further, a deep belief network model based on genetic algorithm is established, which improves the noise resistance through the binary features of neurons in each layer of the DBN, and at the same time, utilize the global optimization searching of the genetic algorithm to identify the optimized structure parameters of the Deep Belief Network (DBN) with consideration of the input data feature collection. This behavior is conducted for the implementation of the fault detection of the generator excitation system. Through the comparison of the fault diagnosis results got from the three algorithms, we can see that the whole accuracy of the GA-DBN algorithm arrives at a surprising 99%. By comparison, the traditional DBN model possesses a total accuracy of 95 percent when we take the count of wrong diagnoses into consideration. When compared with the traditional shallow intelligence diagnosis method, the method which this paper puts forward can diagnose the fault modes of the generator excitation system more stably and possess a higher degree of accuracy.*

KEYWORDS: *wavelet packet decomposition; GA-DBN; generator excitation system; fault detection*

1 Introduction

The excitation system, which acts as the core control device of synchronous generators, occupies an important place in maintaining the stability of terminal voltage. This thing also possesses a remarkable influence upon the adjustment of reactive power distribution and the

*pw1n21@163.com
https://doi.org/10.65102/is2026579
Published: 30 April, 2026

enhancement of both transient and steady-state stability of the whole electric power system[1]. It acts as a key component for guaranteeing the safe, stable, and reliable operation of large - scale electric power - producing units. Along with modern electric power networks continuously expanding, the combination of renewable energy resources keeps growing, and the parameters of electricity generators get more complicated, the excitation system has high probability to meet various kinds of typical wrong functions in its long time working process. These function breakdowns include turn-to-turn short connections in the excitation winding, open/short connection malfunctions of diodes in rectifier bridges, loss or non-uniformities in trigger pulses, and malfunctions in the synchronization signal circuit[2, 3]. The corresponding fault signals have nonlinear character, non-stationary property, and strong mutual connection. This feature lets it become very difficult for traditional check methods which depend on threshold values and shallow models to effectively pick out weak fault features. Because of this, error diagnosis and missing diagnosis happen very often, hence they bring a serious threaten to the safety and stability of electric power systems[4]. Hence, working out methods that have high accuracy and strong stability for fault checking and characteristic analysis in generator excitation systems is very important. These methods have as their goal the reaching of early malfunction identification and quantitative characteristic depiction, which therefore possess quite important theoretical meanings and engineering value. The carry-out of these methods can promote the intelligent operation and maintenance work of generator units, hence promote the reliability degree of power supply[5, 6].

In the passed several years, deep learning has been widely used in the field of power equipment fault check because of its outstanding abilities in independent feature picking and high-dimensional data expression[7]. The Deep Belief Network, which is called DBN for short, it is a classic deep learning model, and it is composed of a number of stacked Restricted Boltzmann Machines that are called RBMs. These RBMs are able to independently obtain high-level features from original signals by utilizing one kind of non-supervised learning method. This method walks around the subjectivity and shortage that connect with manual feature picking. Therefore, hence, the DBN is very suitable to be used for fault pattern recognition in the complex and changeable work environments[8]. Nevertheless, the effect that a standard Deep Belief Network (DBN) has is greatly dependent on the artificial setting of structure parameters, which include the number of hidden layers, hidden nodes, and the study speed. This manual choosing frequently causes the algorithm to be caught in partial optimal solutions, possesses insufficient anti-noise ability, and has a lowered generalization ability. As the result, therefore, it has difficulty in satisfying the requirements of situations which have many faults and strong disturbance in excitation systems. For conquering these restrictions, the union of intelligent optimization arithmetic methods and deep-learning models has hence appeared as an outstanding research field. In the middle of these algorithms, the Genetic Algorithm (GA) has outstanding performance because of its excellent global optimization search capability. It has the ability to independently carry out optimization work on the network framework and super parameters which belong to the DBN. This point, as a consequence, greatly promotes the effectiveness of feature extraction and the accuracy of fault type classification[9, 10].

At the same time, the pre-processing of signals and the extraction of features are necessary requirements for high-quality fault diagnosis. Wavelet Packet Decomposition (WPD) enables the multi-level and meticulous decomposition for both low-frequency and high-frequency components of non-stationary signals. It also can construct sensitive fault feature vectors through the calculation and reconstruction of the energy of each frequency band[11]. This method can accurately depict the waveform distortion and energy distribution characteristics of the exciting current and armature current at the time when a fault takes place. It provides high-quality input characteristics for the afterward deep-learning models[12].

In view of the above-mentioned requirements and difficulties, this paper proposes a novel fault detection method for generator excitation systems. This method is built upon Wavelet Packet Decomposition and a Deep Belief Network which is optimized by the Genetic Algorithm (GA - DBN)[13]. FAt first, a detailed narration is provided by us on the structure and working principle of the static self-excited excitation system. After that, we have performed an analysis which is about the mechanisms of those common faults. These conventional problems include turn-to-turn short connections in the excitation winding together with wrong works in the rectifier circuit[14]. After that, the method of Wavelet Packet Decomposition (WPD) is utilized by us to carry out the decomposition work on the excitation current and the three-phase armature current. According to the sub-band energy, multi-dimensional fault feature vectors are next constructed. Furthermore, the Genetic Algorithm (GA) is utilized by us to carry out a global optimization work for key parameters of the Deep Belief Network (DBN), for example the quantity of hidden nodes and the learning speed rate. This procedure has the objective of constructing an improved DBN model which displays strong adaptive capability and high classification correct rate. At last, simulation experiments have been done under many different working conditions, and a comparison check is completed with traditional calculation methods. The result experiments indicate that the method put forward possesses clear superiorities on the aspects of diagnosis correctness, convergence velocity, and anti-disturbance capability. This can provide theoretical support and technical reference materials for the intelligent fault diagnosis work of generator excitation systems[15, 16].

2 Method

The study first introduces the composition and working principle of the excitation system in detail, and then combines the method of signal processing with deep learning, selects the fault characteristics of the excitation winding turn-to-turn short-circuit and the rectifier circuit fault, and studies the fault classification process based on signal processing. Subsequently, an improved deep confidence network (DBN) method is proposed, which adopts a genetic algorithm to globally search for an optimal DBN network structure and avoids repeated manual debugging of structural parameters. Subsequently, the method of this paper is applied to the generator excitation system fault detection experiments, and the safety and reliability of the method of this paper is verified through example analysis.

2.1 Generator excitation system structure and working principle

We may take the self-excited static excitation system for one example. The constituent elements of the excitation system include the excitation transformer, the excitation controller, the excitation power device, the extinction system, and other such components. The working principle of the whole system is that the signals from the generator terminal voltage, stator current and excitation current are input to the regulator. The working principle of the whole system is just as follows: Signals including generator end voltage, stator electric current and excitation electric current are sent into the excitation regulator. This regulator just now produces control signals. It achieves this purpose through considering input signals, the set values, and through a PID synthesis operation. The control signal is passed to the excitation power unit, through the trigger pulse control thyristor conduction angle, the excitation transformer AC input into DC output for the generator rotor to provide excitation current, generator end voltage and other signals change accordingly. The excitation system and generator form a closed-loop control system.

The excitation system that is in the center of control, its core component is the excitation

regulator, and all automatic control strategies are completed by the excitation regulator. Excitation system schematic diagram shown in Figure 1, in order to improve the reliability of the excitation regulator generally adopts a dual-channel structure, consisting of two independent hardware channels, real-time tracking, mutual standby,seamless and no-mistake automatic switching to maintain the stability of the system's operation, each channel can work in the closed-loop automatic regulation of the machine voltage and the closed-loop manual regulation of the excitation current.

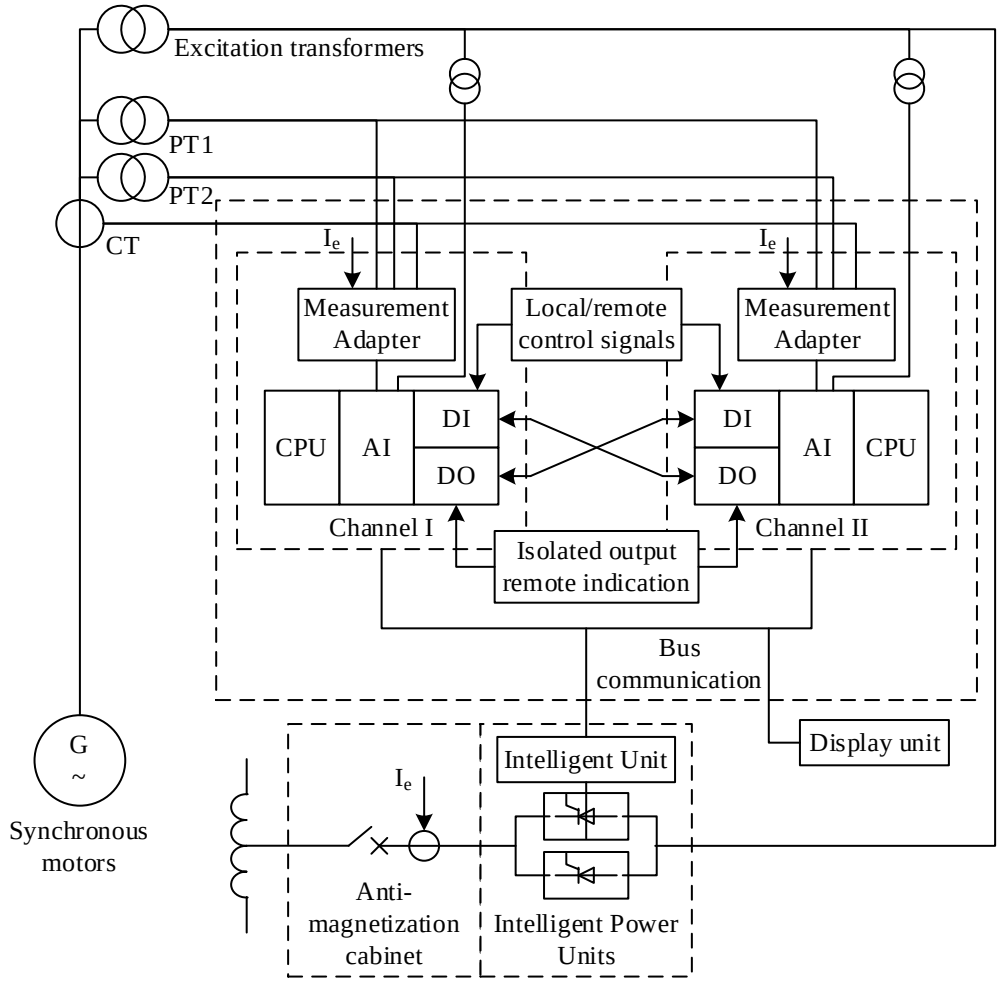

Figure 1: Schematic diagram of excitation control system

At present, there are two kinds of methods that can be used for closing the excitation system to make the magnetization process stop. Under normal situations, the inverter of the full-control bridge rectifier circuit can be used to send back the magnetic field energy of the generator to the generator's stator side. Through this method, the demagnetization work is completed. The employment of reversed electric demagnetization can, in a certain measure, reduce the burden on the machinery demagnetization switch. Under the situations when the generator stops work in abnormal way, for example when a phase-to-phase short circuit or a ground fault takes place either on the inside or on the outside of the generator, fast demagnetization is completed by means of the demagnetizing switch. The demagnetizing switch, it transfers the energy which is stored inside the excitation winding through the energy-consuming components that are within the demagnetizing circuit. This measure is used for prohibiting over-high voltage from appearing inside the excitation winding, which therefore has the possibility to cause harm to the generator. The scheme sketch of the demagnetizing loop is given in Figure 2. In the figure,

R is the demagnetizing resistance, QM is the demagnetizing switch, I_f is the excitation current, and U_f is the excitation voltage. When the degaussing switch operates, the excitation winding forms a closed circuit with the degaussing resistor through the normally closed contacts of the degaussing switch, and the energy of magnetic field that is inside the winding is dissipated through the degaussing resistor R. The demagnetization resistance R may possess either a linear or a non-linear property, which is decided by the generator's structure and its particular application situation.

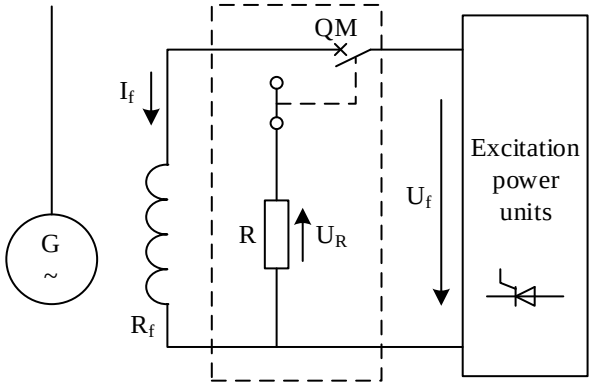

Figure 2: Schematic diagram of de excitation circuit

In current large-scale synchronous generator static excitation systems, the power component is normally a three-phase bridge thyristor rectifier circuit. This selection is under the influence of the generator's ability and the requirements for dependability, the excitation power unit is usually configured for single to four-bridge parallel operation. Many faults in the excitation system, such as synchronization signal circuit faults, trigger pulse faults, fuse faults, thyristor faults, etc. are manifested in the rectifier bridge output waveform abnormality, and the phenomenon of output waveform variation is different between the single-bridge and double-bridge or more parallel structures.

2.2 Fault feature extraction technique based on wavelet packet decomposition

Fault classification requires processing of raw signals to obtain fault characterization information. The main signal handling method that this research paper uses is wavelet packet decomposition.

2.2.1 Principle of wavelet packet decomposition

Wavelet packet decomposition can decompose the low-frequency and high-frequency parts of the signal, and divide the signal into multiple bands of information. Wavelet packet decomposition has two main steps, the first step is to select the appropriate wavelet base, carry out convolution processing through making use of the decomposition of the low-pass filter and the decomposition of the high-pass filter, and then use the downsampling decomposition to get the low-frequency and high-frequency parts of the signal, and then repeat the above decomposition operation, the signal will be processed to the next layer to obtain new bands, and get the information of more frequency bands. After completing all the decomposition steps, the structure of the overall decomposition is the decomposition tree, and all the decomposition coefficients of the low frequency and high frequency can be obtained at the same time. Where the two-scale equation after decomposing the wavelet packet is:

$$\phi(x)=\sum_{k}h(k)\phi(2x-k) \tag{1}$$

$$\varphi(x)=\sum_{k}g(k)\varphi(2x-k) \tag{2}$$

where: $h(k)$ is the decomposed low-pass filter coefficient. $\phi(2x-k)$ is the scale space of the previous layer. $g(k)$ is the decomposed high-pass filter coefficients. $\varphi(2x-k)$ is the wavelet space of the previous layer.

The following stage includes the reconstruction work. According to the wavelet packet decomposition tree structure which is obtained after the previous step is finished, this operation uses a fitting filter. It then according to system traces the wavelet packet decomposition coefficients of each node from the nodes of the decomposition tree back toward the initial signal.After that, according to the tracked moving path, one section inserting calculation work is performed. This operation requires that one carry out a backward convolution calculation, until the number of sampling points of the original signal is completely reconstructed. When all the above-mentioned operations have been completed, the whole reconstruction process will reach its termination.

Each node has a corresponding energy, reconstructing the decomposition coefficients of the last layer of nodes, the subband signals can be obtained, and then the energy $E_1, E_2, \ldots, E_j$ of each subband signal separately is available:

$$E_j=\int\left|S_j(t)^2\right|dt=\sum_{1}^{n}x_j(k)^2 \tag{3}$$

where: $S_j(t)$ is the original signal, x_j is the amplitude. E_j is the node energy.

2.2.2 Signal processing based fault classification process

The original signal after signal processing contains a lot of new information, among which there can reflect the characteristic information under the fault mode. Such as wavelet packet decomposition reconstruction of the energy information of each node. Based on the above feature information, the fault classification of excitation winding turn-to-turn short circuit and rectifier circuit diode fault can be realized for the electrically excited biconvex generator. The fault signal of excitation winding turn-to-turn short-circuit is excitation current, while the fault signal of rectifier circuit diode fault is three-phase armature current, and the fault classification process based on signal processing is shown in Fig. 3.

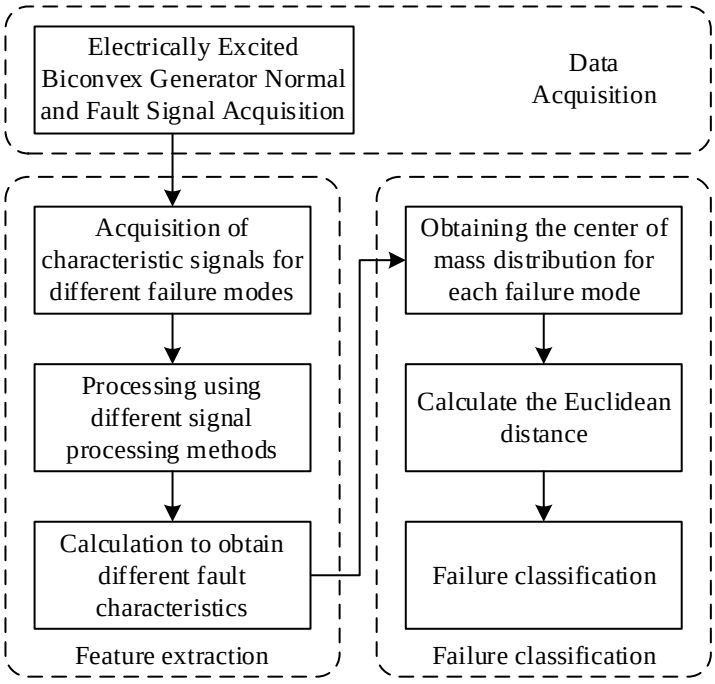

Figure 3: Fault classification process based on signal processing

The specific fault classification steps are:

Step 1: We carry out wavelet packet decomposition processing on the excitation current when the excitation winding has a turn-to-turn short-circuit fault, and on the three-phase current when the rectifier circuit has a diode fault. After that, therefore, the energy value of every single node is got through calculation after the wavelet packet decomposition and reconstruction working process.

Step 2: Firstly, for the case of a certain fault mode, the data obtained are used to construct the feature vector t for a certain fault mode, then t contains all the feature sets after a certain signal processing under this type of fault, which is a one-dimensional vector, and each of the three signal processing modes corresponds to a one-dimensional vector t after processing the original signal.

$$t = \left[x_1(t), x_2(t), \ldots, x_n(t) \right] \tag{4}$$

Step 3: According to the method of constructing feature vectors t in the second step, the feature vectors of the excitation current under the four fault modes of excitation winding turn-to-turn short-circuiting are calculated in turn, which are recorded as $t_i\left(t_1, t_2, t_3, t_4\right)$, and then the four feature vectors are analyzed comparatively and the ones which have some difference in value size in the horizontal coordinates are taken as a fault feature. The four feature vectors are then compared and analyzed, and the one with the same horizontal coordinates and a certain difference in value size can be taken as a fault feature, based on which n fault features can be obtained to form a multidimensional fault feature vector T, and the one-dimensional vector t obtained by the three signal processing modes will be processed again to obtain a multidimensional vector T.

$$T = \left[x_{n1}(t), x_{n2}(t), \ldots, x_{nn}(t) \right] \tag{5}$$

For rectifier circuit diode faults, the three-phase currents under the five fault modes are computed according to the above steps by calculating their respective multidimensional eigenvectors, which are denoted as T_a, T_b, T_c, and then the three-phase armature currents are summed and averaged to obtain the eigenvectors T_a, T_b and T_c are then summed and averaged to obtain the feature vector T, and a multidimensional vector T is obtained for each of the three signal processing methods. This multidimensional fault feature vector T can be used in the subsequent fault classification.

Step 4: After obtaining the multidimensional fault feature vectors, the classification of faults is realized using an improved deep belief network method. The method first utilizes certain training samples to generate thresholds for different fault modes that can be discriminated, and the thresholds are obtained by calculating the average of the Euclidean distance (ED) of the training samples. There are four interval values for excitation winding turn-to-turn short circuits and five threshold values for rectifier circuit diode open faults. Then the Euclidean distance of the test samples is calculated and the fault classification can be achieved by comparing the obtained results with the fault dictionary generated after calculating the thresholds of the training samples.

2.3 GA Optimized DBN Algorithm

2.3.1 DBN structure

DBN consists of a stack of multiple Restricted Boltzmann Machines (RBMs) and a layer of BP network, and the DBN structure is shown in Fig. 4.

A RBM is one type of neural network that is constituted by two layers: one visible layer and one hidden layer. The hidden layer of a single RBM serves as the visible layer of the next RBM, hence these RBMs are piled in order.

$$h = \omega v + b \tag{6}$$

$$v = \omega^T h + a \tag{7}$$

where: v, h are the state vectors of the visible layer and hidden layer. a, b is the visual layer, hidden layer bias vector. ω is the weight vector between the visible and hidden layers.

The RBM stacked network is unsupervised training to reconstruct the input high-dimensional features into low-dimensional features, and initially determine the number of layers, neurons, weights and other parameters of the DBN.The BP network according to the labeling information supervised reverse fine-tuning of the DBN's weights, bias parameters, so as to make the model performance more optimal. Therefore, DBN learning is divided into two processes: feature reconstruction and parameter fine-tuning.

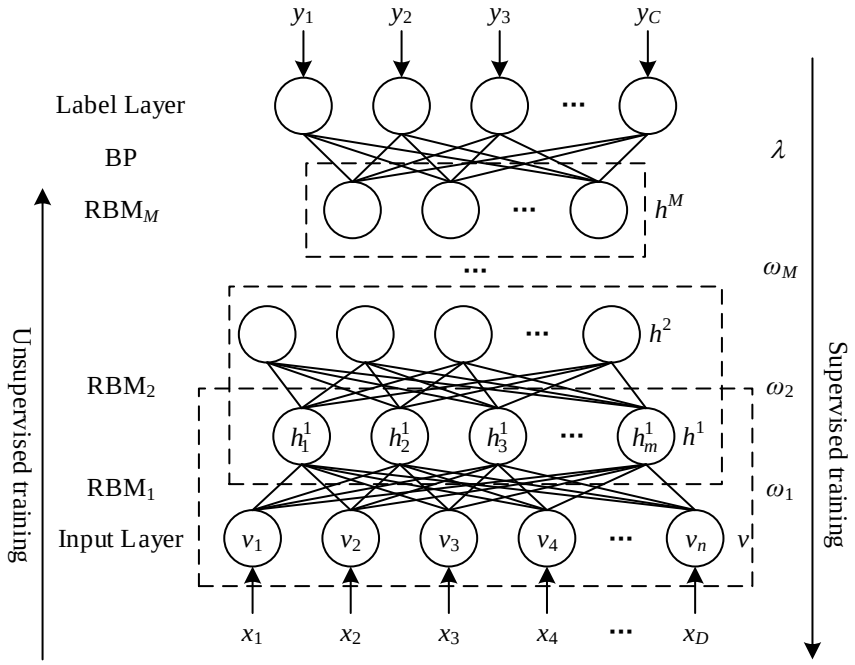

Figure 4: Structure of DBN

2.3.2 DBN feature reconstruction

The basic principle of DBN feature rebuilding includes adjusting the active condition of every nerve cell in the hidden layer. The goal is to make it align as much as can be with the probability distribution that the visible layer has. Furthermore, the number of nerve cells in the hidden layer is maintained to be not greater than that in the visible layer. This arrangement makes certain that the reconstruction process can effectively decrease noise and lower the dimension number.

In the RBM structure, each layer has independence, and the conditional probabilities of neuron activation in the hidden layer and the visual layer are respectively

$$P\left(h_j = 1 \mid v, \theta\right) = \sigma\left(b_j + \sum_i \omega_{ij} v_i\right) \tag{8}$$

$$P\left(v_i = 1 \mid h, \theta\right) = \sigma\left(a_i + \sum_j \omega_{ij} h_j\right) \tag{9}$$

where: $\theta = (a, b, \omega)$ is the RBM model parameter. i denotes the i th neuron in the visual layer. j denotes the j th neuron in the hidden layer. σ is the activation function, the sigmoid function is used in the text.

The joint energy function $E(\mathbf{v}, \mathbf{h} \mid \boldsymbol{\theta})$ between the n visible neurons and the m hidden neurons is

$$E(v, h \mid \theta) = -\sum_{i=1}^{n} a_i v_i - \sum_{j}^{m} b_j h_j - \sum_{i=1}^{n} \sum_{j=1}^{m} v_i \omega_{ij} h_j \tag{10}$$

The RBM model needs to determine the θ value, which can be obtained by inputting the maximum likelihood probability on the training set:

$$\max P(v \mid h, \theta) = \sum_{h} e^{-E(v,h|\theta)} \tag{11}$$

With Gibbs sampling, the RBM uses a contrast scattering algorithm to update the parameters with weights ω_{ij}.

$$\omega_{ij} = \vartheta \omega_{ij} + \varepsilon \frac{\partial \log P(v)}{\partial \omega_{ij}} \tag{12}$$

where: ϑ is the momentum. ε is the learning rate. The update of a_i, b_j is similar to ω_{ij}.

2.3.3 DBN parameter fine-tuning

Each sample $X = \{x_1, x_2, x_3, \cdots, x_D\}$ corresponds to a label $Y = \{y_1, y_2, y_3, \cdots, y_C\}$. D is the number of features and C is the number of sample categories. The label output layer adopts Softmax regression layer, taking the binary classification problem $Y = \{y_1, y_2\}$ as an example, the functional relationship is shown in Eq. (13).

$$y_\lambda(h) = \frac{1}{e^{\hat{y}_1^T h^M} + e^{\hat{y}_2^T h^M}} \begin{bmatrix} e^{\hat{y}_1^T h^M} \\ e^{\hat{y}_2^T h^M} \end{bmatrix} \tag{13}$$

where: λ_1, λ_2 is the weight vector between the sub-top and top layers. h^M is the M th hidden layer vector.

When using the label information to supervised backward fine-tune the whole model parameters, the sample input data is forward propagated to get the model output value. The error is calculated by setting the cost function according to the gap between the model output and the real label.

$$\mu = \frac{1}{N} \sum_{i=1}^{N} \left(y_i^* - y_i \right)^2 \tag{14}$$

where: μ is the mean squared error. y_i^* and y_i are the true label and model output, respectively. N is the sample size of the dataset.

With the goal of minimizing μ, the gradient descent method is utilized by us to optimize the weight and bias parameters of each layer that is inside a Deep Belief Network (DBN).

2.3.4 GA global optimization search

The working effect of the deep neural network model on classification work changes based on the amount of hidden layer numbers. Along with the increment of the quantity of hidden layers, the classification exactness of the deep neural network model has enhancement. But, when the quantity of hidden layers is increased to above four, both the accurate degree and the generalization capability of the model decrease.Genetic algorithm (GA) can operate directly on structural objects and has efficient global optimization capability, which is suitable for optimizing the structural parameters of complex and diverse deep neural networks. Therefore, GA is used to optimize the DBN network structure.When GA optimizes the DBN, the hidden layer range is set to 1~4. For the ensuring of the high accuracy when we get low-dimensional

features, a searching is carried out for the neuron quantity of each layer in the range from 5 to 30. The quantity of hidden layers and the neuron amount in each layer of the Deep Belief Network (DBN) are obtained through random extraction within the preset scope. These values after that are by coding become a chromosome. We have already completed the setting of the population size. When we carry out the training of DBN, the learning rate of 0.01, the momentum of 0.8, the iteration number of 200, and the dropout rate of 0.3 are utilized by us.The global optimization search of GA takes the classification correctness rate as the fitness value. According to the fitness value of the chromosome of the previous generation population, after selection, crossover and mutation to derive the offspring better population, until the optimal, used for generator excitation system safety state sensing.

3 Results and Discussion

3.1 Generator excitation system fault diagnosis

3.1.1 Generator failure mode analysis

This section of the experiment is based on a three-stage aerogenerator as an example. The three-stage aerogenerator structure mainly consists of three stages: a permanent magnet (PM) subexciter, an alternating current (AC) exciter, and a main generator, with each stage containing stator and rotor parts. The normal operation of the generator requires an automatic regulator module for control, and the automatic regulator module contains a rectifier and a proportional-integral (PI) regulator. The regulator module rectifies the three-phase alternating current of the permanent magnet exciter into direct current to provide excitation for the alternating current exciter through the rectifier, in addition, this method can find out the root-mean-square (RMS) value of the output line voltage that the main generator produces, and then compares it with the reference voltage, and then adjusts the alternating current of the alternating current exciter by the error generated by the PI series correction link, so as to realize the control of the voltage of the main generator and ultimately to achieve the purpose of voltage stabilization. The rotary rectifier is located between the AC exciter and the main generator, and its function is to rectify the three-phase AC voltage of the AC exciter in order to provide the main generator's excitation current Ip. Under this background, the fault types of the air generator which are found by the fault feature extraction method that depends on wavelet packet decomposition include the normal type (a non-fault type which can be regarded as a special kind of fault type), the single-pipe fault (6 kinds in total), and the double-pipe fault (15 kinds in total). 3 types (15 types in total), and the classification of fault modes is shown in Table 1.

Table 1: Classification of fault modes

Failure mode	Faulty diode
Health mode	-
Single-tube failure mode	D_1, D_2, D_3, D_4, D_5, D_6
Double-tube failure mode	D_1D_4, D_2D_5, D_3D_6, D_1D_3, D_1D_5, D_3D_5, D_2D_6, D_2D_4, D_4D_6, D_1D_2, D_2D_3, D_3D_4, D_4D_5, D_5D_6, D_6D_1

3.1.2 Data acquisition

During the actual operation of the generator, the rotating rectifier follows the rotor, resulting in a rotor signal that is not easy to measure. Due to the existence of harmonic armature reaction, AC exciter excitation current can reflect the fault information, and also belongs to the

measurable signal in practical application. Therefore, the AC excitation current can be used as an information source.

Figure 5 has given the waveform graphs of the excitation current that belongs to the AC exciter when five kinds of characteristic fault working situations occur. Speak concretely, Figure a to Figure e separately show the normal condition, the D1 fault condition, the D1D4 fault condition, the D1D3 fault condition, and the D1D2 fault condition.There is a certain volatility in the internal inductance and resistance parameters of the motor due to temperature rise and other reasons during generator operation. In order to simulate this characteristic, Monte Carlo (MC) analysis is used in the simulation, and a tolerance of 5% is set for the internal inductance and resistance parameters of the generator at each level, and 100 MC analyses are performed for each failure mode. Considering the effect of generator load, the simulation is carried out under no-load, 1.5kW resistive load and 3kW resistive load conditions in this paper. 200 samples were collected for each fault mode under each load condition, and the sampling clock was set to 10 kHz. Here, in order to simulate the effect of load variations on the methodology, a mixture of no-load, 1.5, and 3kW fault class samples were operated together to form the fault samples under random load conditions. The number of samples for each fault mode class under random load conditions remains 100 (randomly selected from the samples under the 3 load conditions).

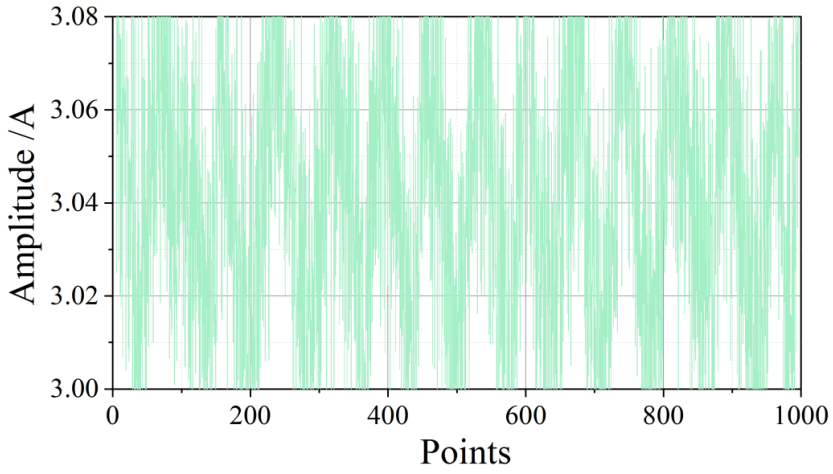

(a) Normal mode

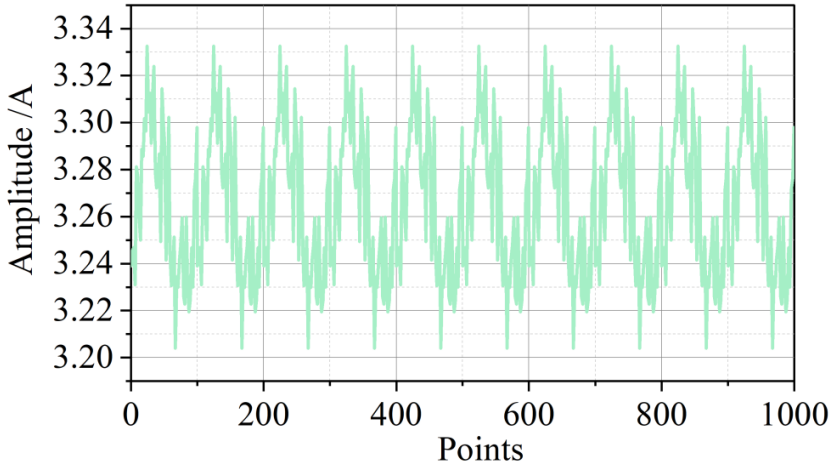

(b) D_1 fault mode

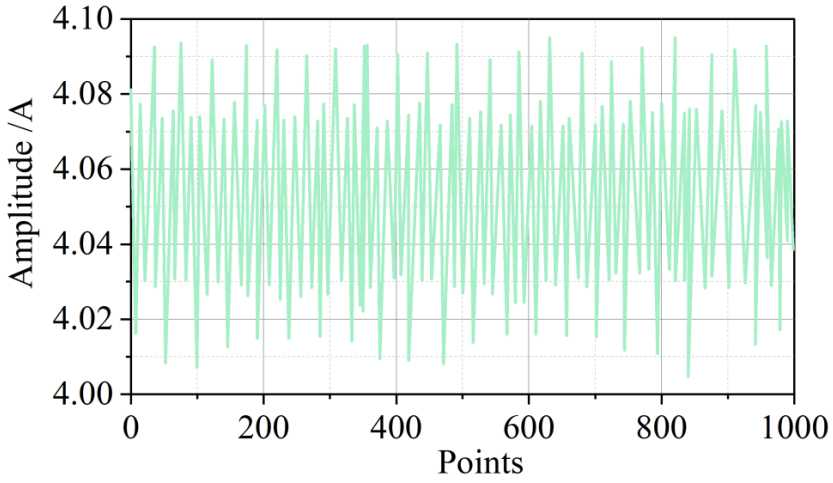

(c) D_1D_4 fault mode

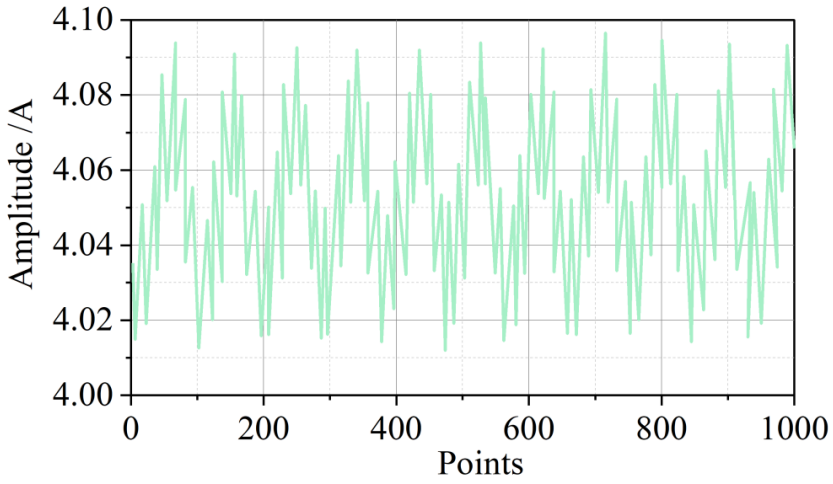

(d)D_1D_3 fault mode

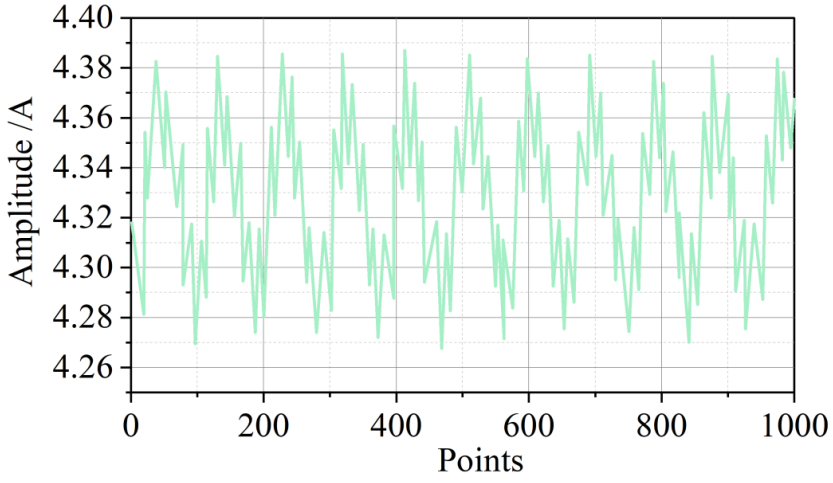

(e) D_1D_2 fault mode

Figure 5: Eive typical fault mode excitation current waveform diagrams

3.2 Example analysis

For the verification of the effect of the method which this paper brings forward (GA - DBN model), hence a diagnostic evaluation is carried out on four fault modes and normal working states of the generator excitation system.Each fault mode is denoted by A to E, respectively. Since the distribution of fault feature vectors is not uniform and the fault modes corresponding to the fault feature vectors are not yet clear, it is not possible to group the fault feature vectors of different categories by the method of equalization. We have selected the K-mean clustering algorithm for the autonomous dividing of feature vectors into different intervals. After that, a separated form of the wrong character vectors for every kind is produced. This discrete form of fault feature vector tables is placed in Table 2, here A to E separately represent the above-mentioned four kinds of faults.

Table 2: Discrete table of fault feature vectors

Symbol	Fault feature vector	Symbol	Fault feature vector	Symbol	Fault feature vector	Symbol	Fault feature vector	Symbol	Fault feature vector
A1	[-4.66,-3.52)	B1	[-2.2,-1.1)	C1	[-3.5,-2.1)	D1	[-2.69,-1.85)	E1	[-0.2,0.1)
A2	[-3.52,-3.02)	B2	[-1.1,-0.6)	C2	[-2.1,-1.43)	D2	[-1.85,-1.42)	E2	[0.1,0.23)
A3	[-3.02,0.1)	B3	[-0.6,-0.4)	C3	[-1.43,-0.56)	D3	[-1.42,-0.96)	E3	[0.23,0.28)
A4	0.1,1.39)	B4	[-0.4,0)	C4	[-0.56,0.03)	D4	[-0.96,-0.92)	E4	[0.28,0.8)
A5	[1.39,2.32)	B5	[0,0.11)	C5	[0.03,1.26)	D5	[-0.92,-0.53)	E5	[0.8,1.43)
A6	[2.32,3.02)	B6	[0.11,1.13)	C6	[1.26,1.72)	D6	[-0.53,-0.55)	E6	[1.43,1.96)
A7	[3.02,4.14)	B7	[1.13,1.53)	C7	[1.72,2.26)	D7	[0.55,-0.01)	E7	[1.96,2.59)
A8	[4.14,5.36)	B8	[1.53,1.99)	C8	[2.26,3.26)	D8	[-0.01,2.22)	E8	[2.59,3.51)
A9	[5.36,7.35)	B9	[1.99,2.97)	C9	[3.26,5.29)	D9	[2.22,2.98)	E9	[3.51,4.88)
A10	[7.35,8.01)	B10	[2.97,3.22)	C10	[5.29,6.5)	D10	[2.98,3.66)	E10	[4.88,6.58)

Setting the minimum support and minimum confidence of the model, the discretized feature vectors are analyzed by Apriori algorithm, and the minimum support and minimum confidence of the model and the failure mode are taken as the conditions, and the minimum support is set to be 8%, and the minimum confidence is set to be 50%. In this paper, we take class 2 faults as an example, and the correlation results are shown in Table 3.

Table 3: Associated result

Range marker	(Support level, confidence level)
A1	(10%, 78.9536%)
B2	(6.6673%, 90.9185%)
B6	(3.3335%, 71.4225%)
A4, C5	(10%, 96.85%)
C5, D8	(10%, 100%)
A4, D8, E1	(6.6278%, 100%)
A4, C5, D8, E1	(6.6278%, 100%)

Table 4 gives the parameter setups for selecting the number of nodes in the hidden layer. In the table, hbest and hbest_2 are the optimal number of RBM1 and RBM2, respectively. The optimal learning rate parameter selection is set as shown in Table 5.

Table 4: Selection and setting of the parameter for the number of nodes

RBM	The initial number of implicit layer nodes	Step length	The number of hidden layer nodes is the maximum
RBM1	1	2	100
RBM2	1	1	hbest
RBM3	1	1	hbest_2

Table 5: Selection and setting of the optimal learning rate parameter

RBM	Initial learning rate	Step length	Maximum learning rate
RBM1	0.012	0.012	1.8
RBM2	0.012	0.012	1.2
RBM3	0.002	0.002	0.3

The training errors corresponding to different numbers of hidden layer nodes are shown in Fig. 6, and Figs. a~c denote RBM1, RBM2, and RBM3, respectively.

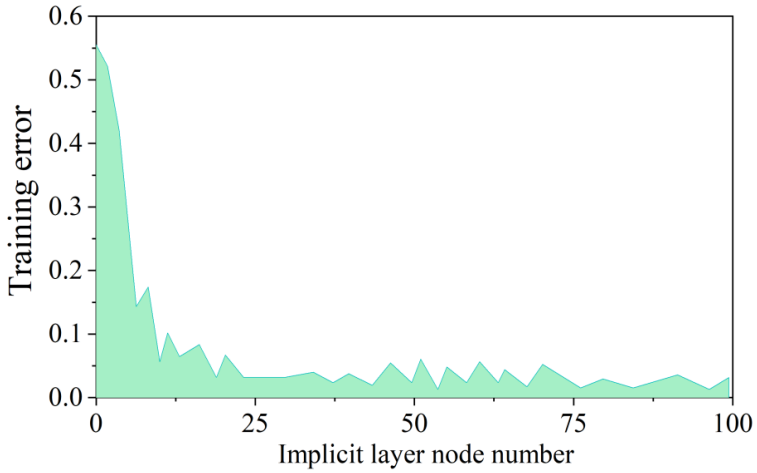

(a) RBM1

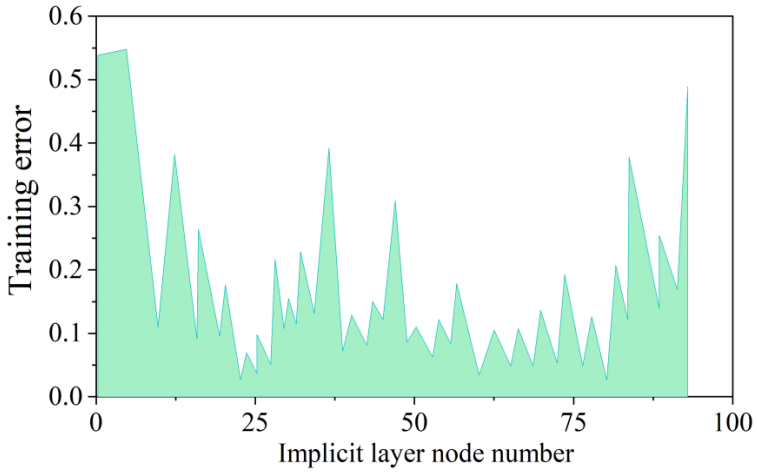

(b) RBM2

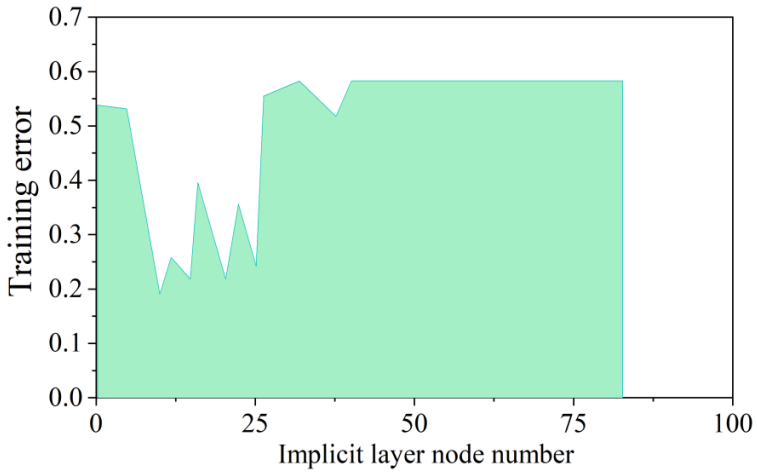

(c) RBM3

Figure 6: The training mistakes that are related to the number of node in different hidden layer

The training errors corresponding to different learning rates are shown in Fig. 7, and Figs. a~c denote RBM1, RBM2, and RBM3, respectively.

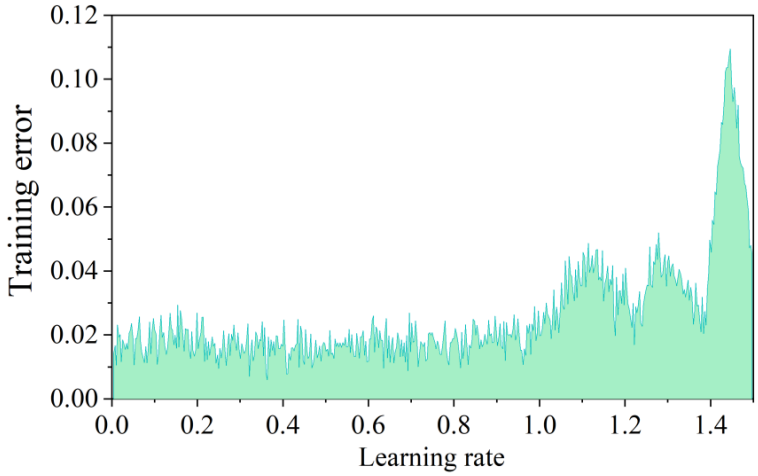

(a) RBM1

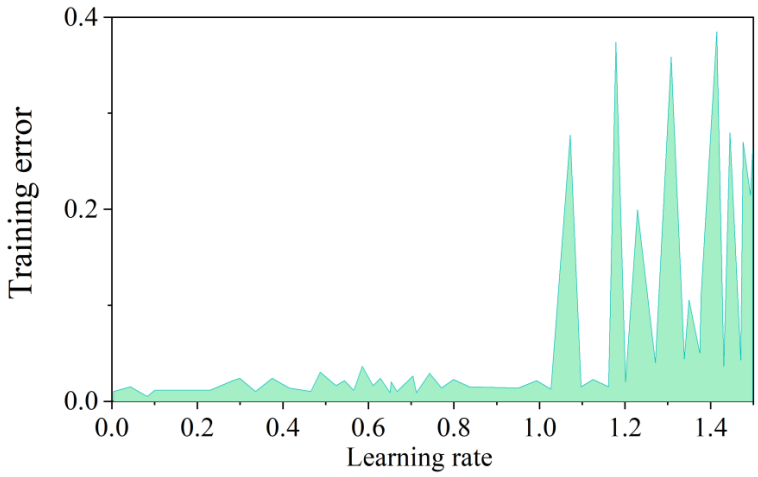

(b) RBM2

(c) RBM3

Figure 7: Training errors corresponding to different learning rates

After iterative calculations to finalize the 3 RBM optimal number of hidden layer nodes and optimal learning rate, the optimal number and learning rate are shown in Table 6, that is, the DBN is 5-95-46-22-10 structure.

Table 6: Optimal number and learning rate

RBM	The optimal number of hidden layer nodes	Optimal learning rate
RBM1	95	0.85
RBM2	46	0.31
RBM3	22	0.07

DBN model, LM neural network model and GA-DBN model are also selected for comparison. The learning rate comparison is shown in Fig. 8, Fig. a for DBN and Fig. b for this paper's model. The standard DBN sets the initial learning rate as 0.5,and the minimum value of the learning rate is 0.001.When the adaptation is smaller than the optimal adaptation of the previous generation, the learning rate is halved until it is smaller than the minimum value to

end the cycle.GA-DBN adopts the optimal learning rate. From the figure, it can be seen that the standard DBN reaches the minimum value of learning rate in the 93rd time, and the GA-DBN reaches the minimum value of learning rate in the 50th time, so the GA-DBN has a faster, less iteration and faster iteration speed.

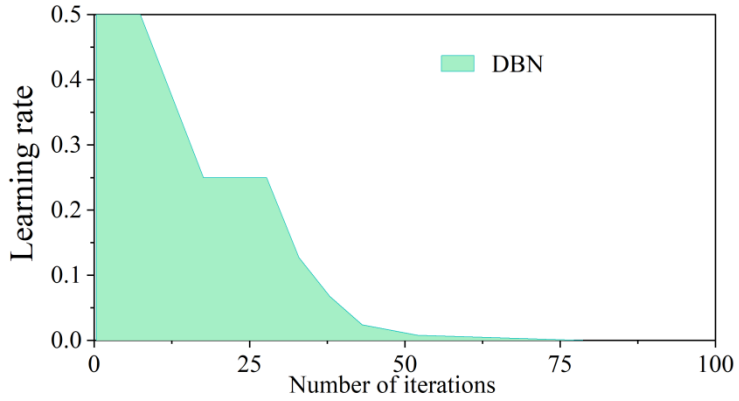

(a) DBN

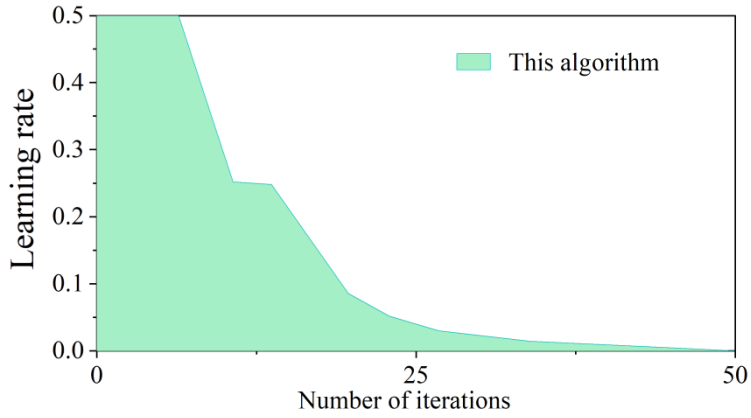

(b) This algorithm

Figure 8: Comparison of learning rates

The comparison of the fault diagnosis results of the three algorithms is shown in Fig. 9, (a)~(c) are the diagnosis results of the model in this paper (GA-DBN), the diagnosis results based on the DBN model and the diagnosis results based on the LM model, respectively. In addition, the number of GA-DBN misdiagnosis is 3 out of 300 test data, and the overall accuracy can be as high as 99%.In the same group of test data, the standard DBN model has 15 wrong diagnoses, and its whole correct rate is 95%. It is obvious that, when compared with the traditional shallow intelligent diagnosis method, the method which is proposed in the present paper can realize the diagnosis of fault patterns of generator excitation system in a more stable way and with higher accuracy.

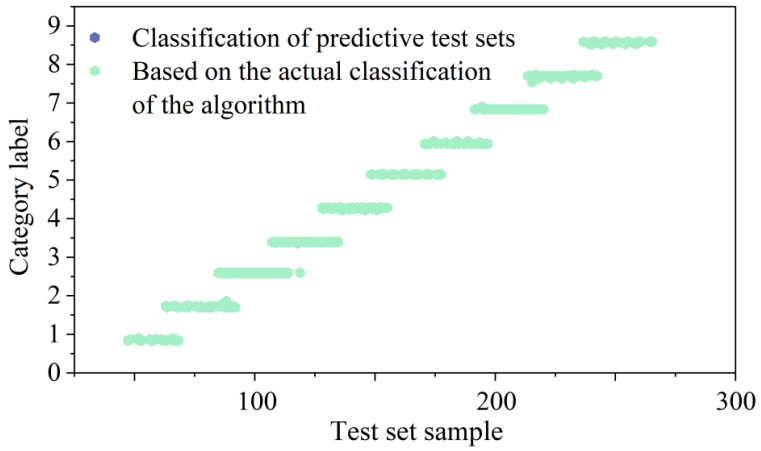

(a) This algorithm

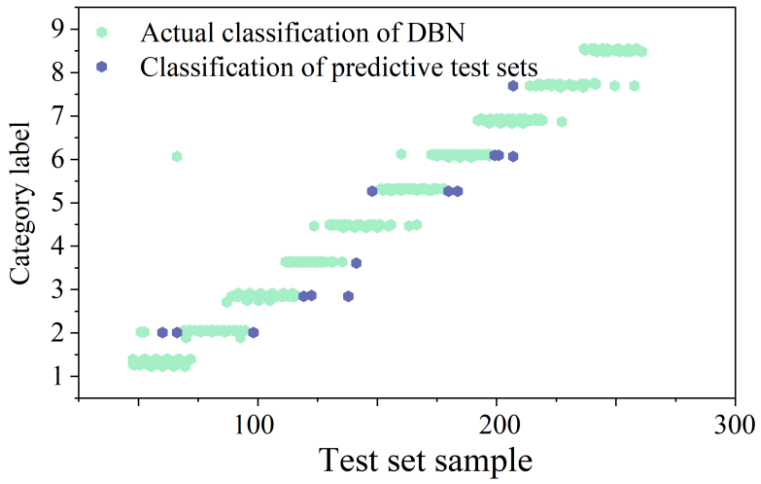

(b) DBN result

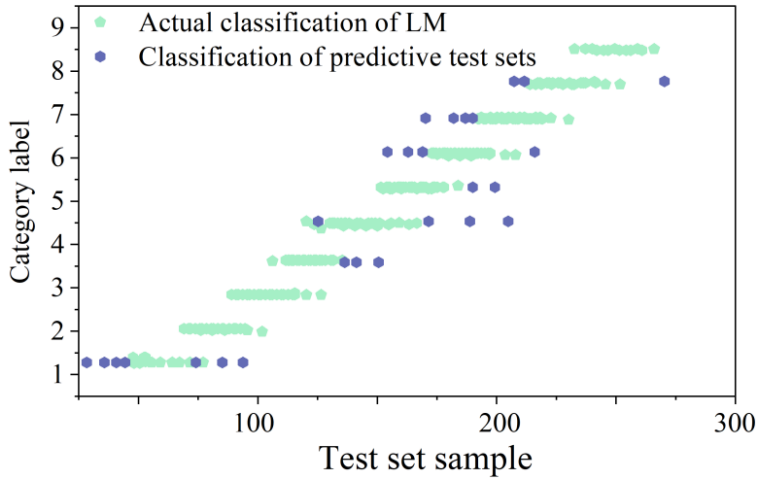

(c) LM result

Figure 9: Fault diagnosis result

4 Conclusion

In order to improve the safety and reliability of generator excitation system, the study explores the fault feature extraction method based on wavelet packet decomposition and the fault classification method of generator excitation system based on improved deep confidence network. The experimental conclusions of this paper are:

(1) The fault patterns of the aviation electricity generator which are recognized by the fault feature extraction method which is built upon wavelet packet decomposition include three kinds: normal working patterns, single-line faults (altogether six types), and double-line faults. This shows that the fault feature extraction method which is based on wavelet packet decomposition that is put forward in this paper is an effective method for extracting fault features. Furthermore, it has given out good results in both simulation works and experiment works.

(2) When we make comparison between the DBN model and the LM neural network model, the fault detection precision of the strengthened deep belief network put forward in this paper has been obviously promoted. In very many experiments, the accuracy can surpass 99%, which is the highest value among the three models. This proves the better property of the model's effect in this paper.

Funding

Project supported by Science and Technology Project of Zhejiang Energy Group (ZNKJ-2022-078).

References

[1] Lu, Q. Z. (2025). Design of Generator Excitation System Fault Detection System Based on Cloud Computing. Electrical Engineering and Economy, (6):304-306+311.

[2] Shi, C. S. (1999). Fault Detection Method for Excitation Voltage Regulation System of Yangtze Series Gasoline Generator Sets. Mobile Power Supply & Vehicle, 30(2):34-35.

[3] Du, C. K., Zhu, D. L., Yang, G. Q., & Wang, T. X. (2008). Research on DSP-based Dual-Microcomputer Excitation Fault Detection and Automatic Switching System. Guangxi Electric Power, 31(6):1-5+17.

[4] Hao, L. L., Sun, Y. G., Qiu, A. R., & Wang, X. H. (2011). Steady-State Fault Feature Analysis of Inter-turn Short Circuit in Excitation Winding of Large Hydro-generator. Automation of Electric Power Systems, 35(4):40-45.

[5] Duan, J. D., Chen, J. L., & Xie, Y. H. (2016). Adjustment Characteristic Analysis of Excitation Regulator After Removal of External Generator Faults. Electronic Measurement Technology, 39(11):60-64.

[6] Gui, G. L., Dai, S. H., & Chen, Y. Y. (2009). Fault Analysis of Measurement Unit Board of Generator Excitation Regulator. Anhui Electric Power, 26(3):1-4.

[7] Xu, P. Y. (2013). Analysis of Two Faults of Generator Excitation Regulator. Electric Power Safety Technology, 15(10):52-53.

[8] Hui, H. (2021). Fault Analysis of Synchronous Generator Excitation Regulator. Electric Engineering, (2):53-54.

[9] Cui, J., Guo, R. D., Zhang, Z. R., Wang, L., & Meng, S. S. (2020). Improved DBN-based Fault Feature Extraction Technology for Generator Rotating Rectifier. Proceedings of the CSEE, 40(7):2369-2376.

[10] Lei, Z., Xin, Z., & Ke, Y. (2025). Incipient fault detection and process monitoring of thermal power plant pulverizing system based on deep representation learning. Transactions of the Institute of Measurement and Control, 47(15):3111-3123.

[11] Tang, X., & Yue, P. (2025). Deep learning-based detection of cascading failure events in power systems using an event-triggered hybrid model framework. Electrical Engineering, 107(12):1-15.

[12] Lin, G., Zhang, H., & Chen, L. (2025). Deep Learning Based Fault Detection and Diagnosis Method for Power Systems. Applied Mathematics and Nonlinear Sciences, 10(1).

[13] Yoon, H. D., & Yoon, J. (2024). Development of a real-time fault detection method for electric power system via transformer-based deep learning model. International Journal of Electrical Power and Energy Systems, 159:110069.

[14] Key, S., Son, W. G., & Nam, R. S. (2024). Deep Learning-Based Algorithm for Internal Fault Detection of Power Transformers during Inrush Current at Distribution Substations. Energies, 17(4):963.

[15] Prasad, S. T. (2023). A deep learning-based protection scheme for fault detection and classification in wind integrated HVDC transmission system under dissimilar fault scenarios and uncertain conditions. Neural Computing and Applications, 35(24):17929-17940.

[16] Awasthi, A., Mahesh, R. T., Joshi, R. (2022). Smart Grid Sensor Monitoring Based on Deep Learning Technique with Control System Management in Fault Detection. International Journal of Communication Networks and Information Security, 14(3):123-137.